

Sunday Driver links axonal transport to damage signaling

Valeria Cavalli,¹ Pekka Kujala,² Judith Klumperman,² and Lawrence S.B. Goldstein¹

¹Department of Cellular and Molecular Medicine, Howard Hughes Medical Institute, University of California, San Diego, La Jolla, CA 92093

²Department of Cell Biology, Universitair Medisch Centrum Utrecht, 3584CX Utrecht, Netherlands

Neurons transmit long-range biochemical signals between cell bodies and distant axonal sites or termini. To test the hypothesis that signaling molecules are hitchhikers on axonal vesicles, we focused on the c-Jun NH₂-terminal kinase (JNK) scaffolding protein Sunday Driver (syd), which has been proposed to link the molecular motor protein kinesin-1 to axonal vesicles. We found that syd and JNK3 are present on vesicular structures in axons, are transported in both the anterograde and retrograde axonal transport pathways, and interact

with kinesin-I and the dynactin complex. Nerve injury induces local activation of JNK, primarily within axons, and activated JNK and syd are then transported primarily retrogradely. In axons, syd and activated JNK colocalize with p150^{Glued}, a subunit of the dynactin complex, and with dynein. Finally, we found that injury induces an enhanced interaction between syd and dynactin. Thus, a mobile axonal JNK–syd complex may generate a transport-dependent axonal damage surveillance system.

Introduction

Intracellular transport of vesicles by molecular motor proteins such as kinesins, dyneins, and myosins is essential for many neuronal and other cellular processes. Kinesins define a superfamily of motor proteins that use the energy of ATP hydrolysis to move cargo toward the plus-end of microtubule tracks. Dynein has an essential role in fast retrograde axonal transport (Paschal and Vallee, 1987) and is known to require the associated protein complex dynactin (Karki and Holzbaaur, 1999). Although kinesins and dyneins transport several classes of cargoes, the organization and properties of the motor protein receptors on such cargoes remain poorly understood.

A genetic screen in *Drosophila melanogaster* for axonal transport mutants led to the discovery of a receptor protein, Sunday Driver (syd), that appears to link conventional kinesin, kinesin-I, to an unknown class of vesicles (Bowman et al., 2000). Other potential kinesin-I receptors identified recently include the amyloid precursor protein (APP; Kamal et al., 2000), the glutamate receptor interacting protein GRIP1 (Setou et al., 2002), and the c-Jun NH₂-terminal kinase (JNK) inter-

acting proteins (JIP), JIP1 and JIP2 (Verhey et al., 2001). The syd protein is homologous to mammalian JIP3 (or JSAP1), which was found in yeast two-hybrid screens for proteins interacting with JNK, also known as stress-activated protein kinase (Ito et al., 1999; Kelkar et al., 2000).

The JNK signaling pathway is implicated in multiple physiological processes, allowing a cell to mount an appropriate response to extracellular stress (Davis, 2000). The stress pathway is organized in a cascade of phosphorylation events, which culminate in the activation of a family of transcription factors, including c-Jun, to regulate gene expression. Three genes encode the JNK protein kinase in mammals. *Jnk1* and *Jnk2* are ubiquitously expressed, whereas *Jnk3* is expressed primarily in the nervous system (Davis, 2000). The JNK signaling pathway mediates neuronal apoptosis in response to stress (Yang et al., 1997) and during development (Kuan et al., 1999). In the injured central nervous system, c-Jun was recently shown to be an important regulator of axonal regeneration (Raivich et al., 2004). JNK has also been implicated in nerve regeneration in the peripheral nervous system (Kenney and Kocsis, 1998). The downstream transcription factor c-Jun is one of the earliest and most consistent markers for neurons that respond to nerve-fiber transection, and its expression in neuronal cell bodies can be related to both degeneration and survival, including target reinnervation (for review see Herdegen et al., 1997).

The finding that multiple types of JNK scaffolding proteins interact with kinesin-I raises the question of whether or not

Correspondence to L.S.B. Goldstein: lgoldstein@ucsd.edu

P. Kujala's present address is the Netherlands Cancer Institute, 1066CX Amsterdam, Netherlands.

Abbreviations used in this paper: APP, amyloid precursor protein; DHC, dynein heavy chain; DIC, dynein intermediate chain; DRG, dorsal root ganglia; JIP, JNK interacting protein; JNK, c-Jun NH₂-terminal kinase; KLC, kinesin light chain; PNS, postnuclear supernatant; syd, Sunday Driver.

The online version of this article includes supplemental material.

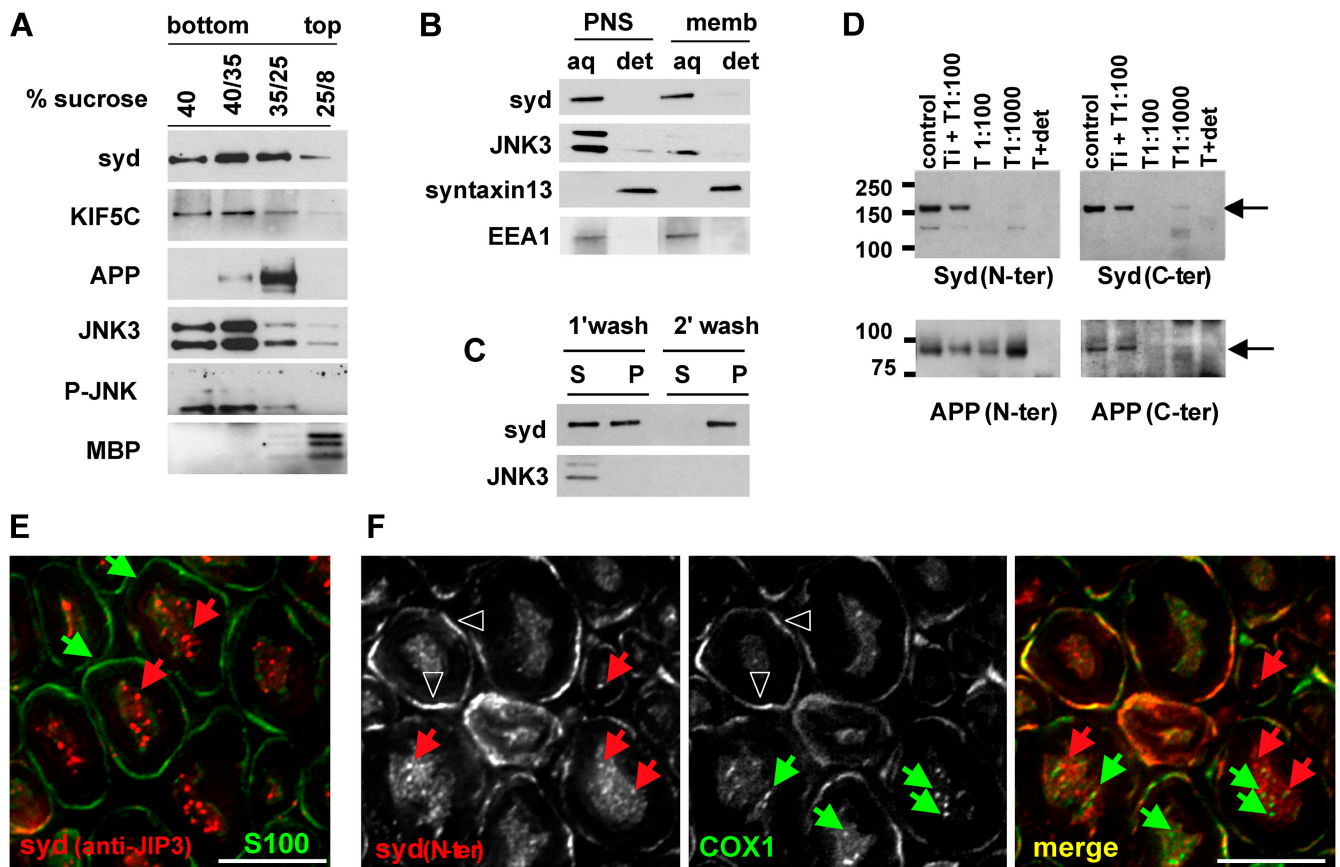


Figure 1. Syd is a peripheral membrane protein associated with axonal vesicular structures in mouse sciatic nerve. (A) After flotation on sucrose step gradients, *syd*, KIF5C, JNK3, and P-JNK are present in both the soluble fraction (40% sucrose) and the membrane fraction (35/25 interface). The 40/35 interface contains both soluble and membrane-bound proteins (note that JNK antibodies recognize the 46- and 54-kd isoforms). (B) Sciatic nerve PNS or floating membrane fractions (*memb*) were treated with Triton X-114 at 4°C. *Syd* and JNK3 are found in the aqueous phase (note that the top band recognizing the JNK3 54-kd isoform is below detection level at this exposure time in the membrane extraction). (C) After carbonate wash of sciatic nerve PNS, a significant amount of *syd* remains associated with membranes. (D) Brain membrane fractions were treated with trypsin (T) in the presence or absence of soybean trypsin inhibitor (Ti) or Triton X-100 (*det*), as indicated. APP is protected from trypsin digestion, whereas *syd* is not detected with NH₂- or COOH-terminal antibodies after digestion. (E) Sciatic nerve cross sections were stained for *syd* (anti-JIP3) and S100, a Schwann cell marker. Deconvolution analysis shows punctate *syd* staining. Red arrows, *syd* puncta; green arrows, Schwann cells. (F) Sciatic nerve cross sections were stained for *syd* (*syd* N-ter) and COX1. No colocalization is observed. Red arrows, *syd* puncta; green arrows, COX1 puncta; arrowheads, myelin outer layer. Bars, 5 μm.

JNK signaling is regulated by vesicular transport (Bowman et al., 2000; Verhey et al., 2001). This question is of particular importance in neurons, where signals are sent in both directions between the cell body and the distantly located nerve terminal. Nerve injury triggers numerous changes in the injured neurons and surrounding nonneuronal cells that ultimately result in successful target reinnervation or cell death. Sciatic nerve transection induces a rapid and prolonged increase in c-Jun activation and transcription in sensory and motor neuron nuclei (Jenkins and Hunt, 1991; Leah et al., 1991) as well as the appearance of activated JNK in the cell body (Kenney and Kocsis, 1998). Most importantly, the amount of time it takes for activated JNK and c-Jun protein to appear in the cell body depends on the distance of the axotomy site from the cell bodies (Kenney and Kocsis, 1998). In addition, JNK has been localized to peripheral nerve axons and is transported both anterogradely and retrogradely (Middlemas et al., 2003). Although these results suggest the existence of a retrograde injury signal that might be initiated by JNK, they failed to identify the nature of the retrograde signal itself and did not reveal if JNK is physically transported from injury sites to cell bodies.

The finding that *syd* interacts with both JNK3 and kinesin-I suggests that this scaffolding protein might target signaling molecules to specific subcellular locations by binding to moving vesicles. However, the data reported so far on JNK scaffolding proteins did not address their subcellular distribution *in vivo* nor did they reveal whether or not JNK might be present in a JIP–kinesin complex (Ito et al., 1999; Bowman et al., 2000; Kelkar et al., 2000). Here, we probe these issues and test directly the hypothesis that *syd*, in collaboration with JNK and the molecular motor system, establishes a vesicular axonal damage signaling system in peripheral nerves.

Results

Syd is a peripherally associated membrane protein

Initial data and motif analysis suggested that *syd* might be a transmembrane protein (Bowman et al., 2000). To test this hypothesis, we performed a detailed biochemical characterization. In sucrose step flotation gradients, in which sciatic nerve extract was bottom loaded, *syd*, together with the motor

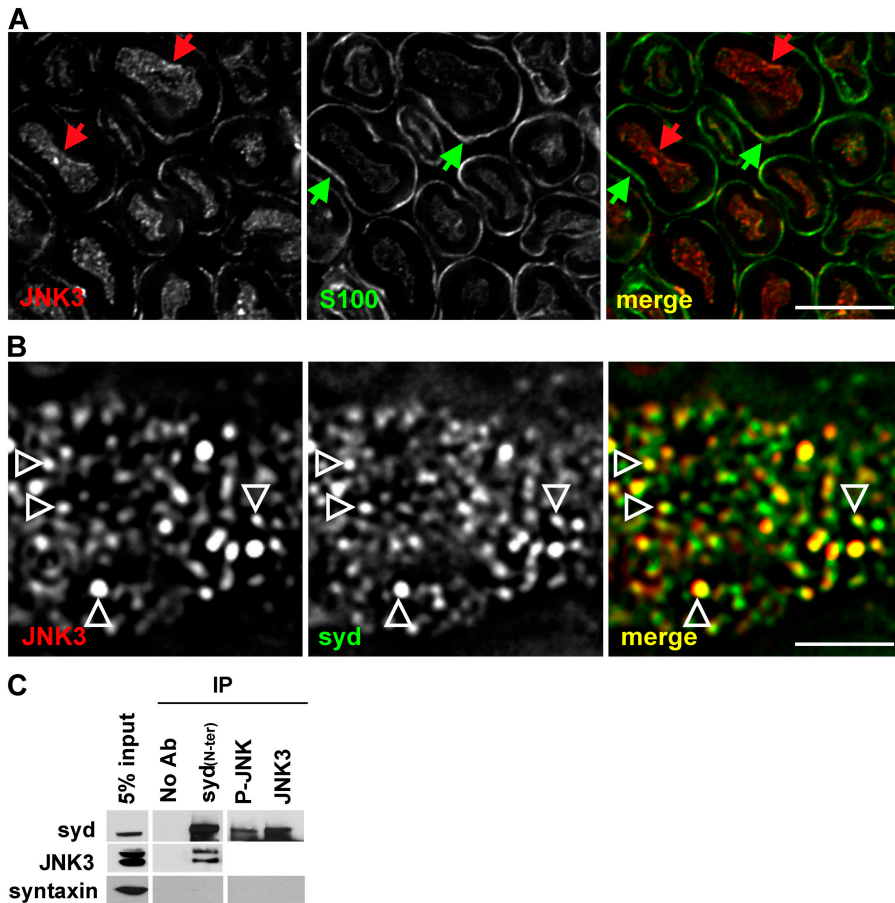


Figure 2. **Syd and JNK3 form a complex in vivo.** (A) Sciatic nerve cross sections were stained for JNK3 and S100. Red arrows, JNK3 puncta; green arrows, Schwann cells. (B) Partial colocalization (arrowheads) is observed between syd and JNK3 puncta in longitudinal sciatic nerve sections within a single axon. (C) Coimmunoprecipitation with syd, P-JNK, JNK3, or no antibodies was performed from brain extract and probed with the indicated antibodies. A fraction of JNK3 is associated with syd (the JNK3 signal for the P-JNK and JNK3 lanes cannot be detected as a result of masking by the IgGs). Bars: (A) 5 μ m; (B) 2 μ m.

protein kinesin-I (KIF5C), was present in both the soluble fraction (40% sucrose) and the different sucrose interfaces that are characteristic of membrane compartments (Fig. 1 A). The transmembrane protein APP is found exclusively in the 35/25 floating fractions, whereas myelin basic protein is found exclusively in the 25/8 interface. Syd is a scaffolding protein for the JNK group of stress-activated protein kinases and shows preferential binding of the neuronal enriched isoform JNK3 over the ubiquitous JNK1 and JNK2 (Ito et al., 1999; Kelkar et al., 2000). Thus, we examined the distribution of JNK3 in the sucrose step gradient. We find a small fraction of JNK3 associated with membrane in the floating fractions. The activated form of JNK, detected with an antibody against the phosphorylated form (P-JNK), is also present in the 35/25 interface.

To test if syd is a peripherally or integrally associated membrane protein, we performed Triton X-114 phase separation (Bordier, 1981; Fig. 1 B). After phase separation, transmembrane proteins are enriched in the detergent phase, whereas soluble and peripherally associated proteins are enriched in the aqueous phase. We found that syd partitions in the aqueous phase, together with JNK3 and early-endosomal autoantigen 1 (EEA1), whereas the transmembrane protein syntaxin13 partitions in the detergent phase. After carbonate wash of sciatic nerve extract, a substantial fraction of syd remains associated with the membrane pellet fraction, in contrast to JNK3, which is completely released in the supernatant (Fig.

1 C). These results suggest that the interaction of syd with membranes is resistant to high pH. We also tested syd location with a trypsin digestion protection assay (Fig. 1 D). A total brain membrane fraction was prepared by sucrose flotation step gradient fractionation and subjected to trypsin digestion. We observed that syd is not protected from trypsin digestion because neither NH₂-terminal- nor COOH-terminal-specific antibodies detect syd after digestion. As a control, the type 1 transmembrane protein APP is shown. As expected, APP is detected after digestion with an NH₂-terminal antibody but not with a COOH-terminal antibody. These results suggest that syd exists in two pools: one soluble and one peripherally associated with membranes. The membrane-associated pool is stable to high pH conditions. A small but significant fraction of JNK3 is also associated with membranes.

To test whether syd is associated with axonal organelles, we performed immunofluorescence on sciatic nerve cross sections. We observed that syd is primarily localized in axons (Fig. 1, E and F). Little colocalization was observed with the Schwann cell marker S100 when the purified anti-JIP3 antibody was used (Fig. 1 E), although some background staining of the myelin outer layer was positive for both COX1 and syd when the crude serum (Fig. 1 F, syd N-ter) was used (Fig. 1 F, arrowheads). Deconvolution analysis revealed that the staining pattern for syd in axons appeared vesicular and no colocalization with the mitochondrial marker COX1 was observed. These results are consistent with the observation

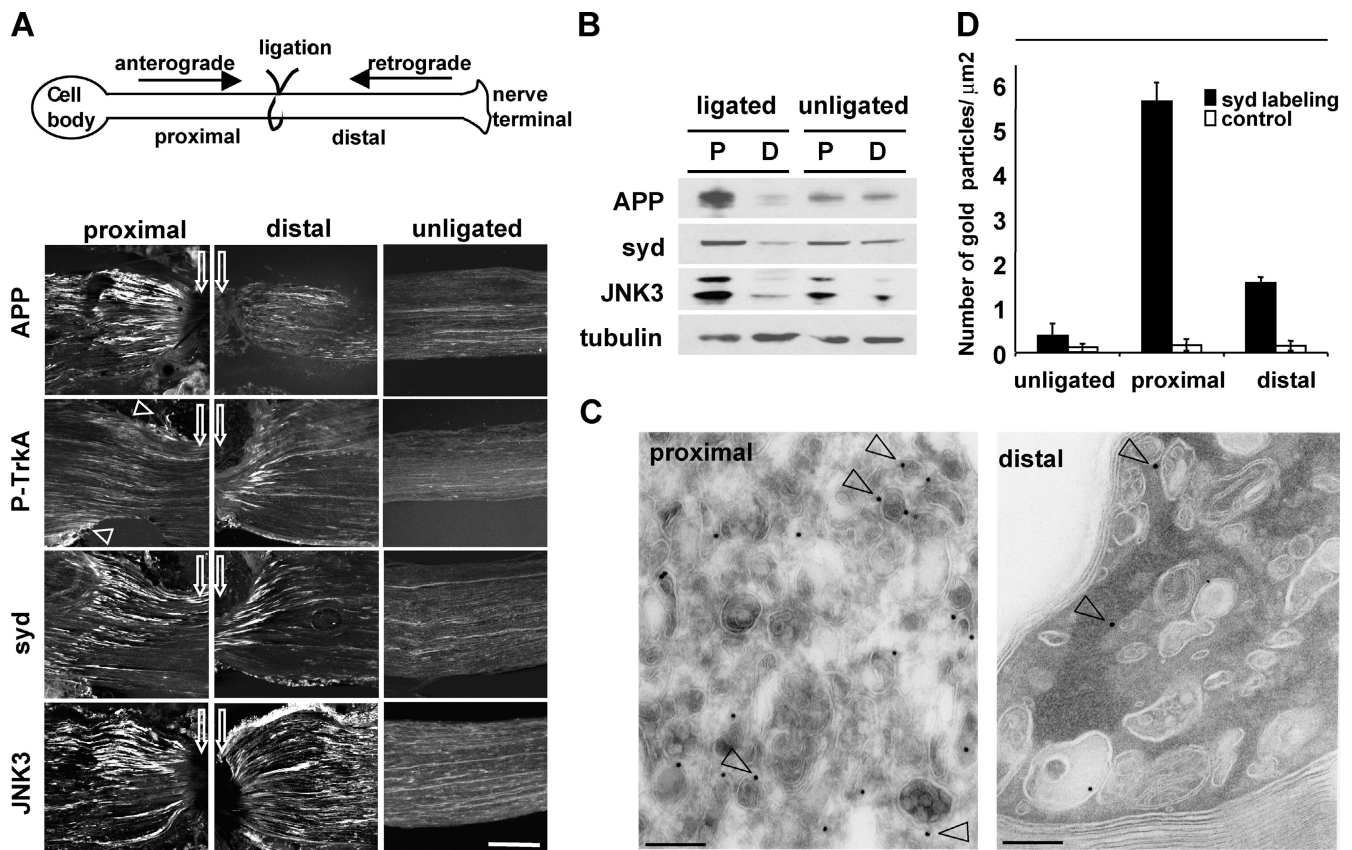


Figure 3. Syd and JNK are transported in both the anterograde and the retrograde pathways. (A) Sciatic nerves were ligated unilaterally at the midpoint and processed for immunofluorescence. APP accumulates primarily on the proximal side of the ligation, whereas phospho-TrkA primarily accumulates on the distal side (arrowheads point to nonspecific staining of the perineurium). Syd and JNK3 accumulate on both proximal and distal sides. White arrows point to ligation site. (B) Ligated and contralateral unligated sciatic nerves were dissected, and extracts were analyzed with the indicated antibodies. Tubulin is used as a loading control. Replicates are shown in the online supplemental material. (C) Sciatic nerve ligation was performed as in A. Nerves were dissected and processed for EM. Proximal and distal sections were stained for syd (15 nm of protein A gold; arrowheads). (D) Total gold particles on an area of 100 μm^2 on both proximal and distal axoplasm and an equivalent area on unligated nerve axoplasm were counted. The results are given as the number of gold particles per square micrometer \pm SEM. Bars: (A) 100 μm ; (C) 200 nm.

that a fraction of syd is biochemically associated with sciatic nerve membranes.

Syd and JNK3 form a complex in vivo

Syd and JNK3 have been shown to interact in vitro, when isolated from cotransfected cells (Ito et al., 1999; Kelkar et al., 2000). Similarly to syd, JNK3 showed a punctate pattern in sciatic nerve axons (Fig. 2 A). These results are in agreement with the observation that a significant fraction of JNK3 is biochemically associated with membrane (Fig. 1 A). To further test whether or not syd and JNK3 are found in a complex in vivo, we performed high resolution imaging of single axons stained with syd and JNK3. There is significant overlap between JNK3 and syd positive puncta in axons indicating that they reside, at least in part, in the same axonal compartment. A complete overlap was not expected because JNK3 also binds other scaffolding proteins, including JIP1, JIP2 (Yasuda et al., 1999), and β -arrestin-2 (McDonald et al., 2000). Next, we performed coimmunoprecipitation from mouse brain extracts. A small but significant fraction of JNK3 can be immunoprecipitated with the syd NH₂-terminal antibody (Fig. 2 C). The reverse experiment shows that syd can be coimmunoprecipitated with antibodies directed

against JNK3 and P-JNK. As a negative control syntaxin is not detected in the coimmunoprecipitations.

Syd and JNK3 are transported in both anterograde and retrograde axonal transport pathways

The direct interaction between syd and kinesin-I (Bowman et al., 2000) suggests that syd should be transported in axons in the fast anterograde pathway. To test this hypothesis, we performed sciatic nerve ligation experiments. Mouse sciatic nerves were subjected to ligatures for 6 h, and nerve portions proximal or distal to the ligation were analyzed by immunofluorescence microscopy and Western blotting (Fig. 3 A; see Materials and methods). Proteins moving in the fast anterograde axonal transport pathway generally accumulate on the proximal side of a ligation, whereas stationary, slow moving, or nonaxonal proteins remain unchanged. Immunofluorescence of longitudinal sections of a ligated nerve revealed accumulation of APP primarily on the proximal side, as shown previously (Fig. 3 A; Kamal et al., 2000). As a marker for retrograde transport, we performed staining for activated phosphorylated TrkA, which, as expected, accumulated on the distal side (Ehlers et al., 1995; Fig. 3 A). Staining with anti-syd NH₂-terminal antibodies revealed that syd accumulates on

Table I. Syd association with membranes is increased by sciatic nerve ligation

Nerve axoplasm	Labeling	Membrane-bound gold particles/total gold
Proximal	syd labeling	92.9% (522 out of 562)
	control	35.3% (6 out of 17)
Distal	syd labeling	85.3% (133 out of 156)
	control	33.3% (5 out of 15)
Unligated	syd labeling	51.4% (19 out of 37)
	control	27.3% (3 out of 11)

Sciatic nerve ligation was performed as in Fig. 3. Nerves were dissected and processed for immunoelectron microscopy. Staining and counting was performed as described in Fig. 3 D. The percentage of the membrane-bound label, i.e., gold particles within a distance of 15 nm or less from the closest membrane profile, was determined.

the proximal side, as expected for a kinesin-I binding protein. We also observed a smaller but significant accumulation on the distal side (Fig. 3 A). Staining with antibodies against JNK3 also revealed accumulation on both the proximal and distal sides (Fig. 3 A), as reported previously (Middlemas et al., 2003).

By Western blot analysis, we observed accumulation of APP on the proximal side and clearance from the distal side (Fig. 3 B; Kamal et al., 2000). Accumulation on the proximal side and clearance from the distal side is also observed for syd. The extent of accumulation is smaller than APP and might reflect the small but significant amount of syd transported in the retrograde axonal pathway. The same was observed for JNK3. Note that the JNK3 levels exhibit some variability in the unligated nerve; however, a consistent proximal accumulation in ligated nerves is evident when these experiments are done several times (Fig. S2 A, available at <http://www.jcb.org/cgi/content/full/jcb.200410136/DC1>). The amount of tubulin, which is transported by slow axonal transport, remains unchanged between ligated and unligated nerves and serves as a loading control.

To test if syd is associated with axonal vesicular carriers, we performed immunoelectron microscopy on ligated sciatic nerves. Organelles accumulating proximal to a ligation are mostly small vesicles, whereas the population of organelles accumulating distal to a crush contains large diameter organelles, many of them dense lamellar bodies, and also small vesicles (Tsukita and Ishikawa, 1980). We found that syd is localized on the proximal side to small vesicles/tubules as well as to larger-sized carriers (Fig. 3 C). Although the syd-positive carriers often contained internal membranes, syd label was restricted predominantly to the limiting membrane, which is consistent with a role of syd in kinesin-I-based transport. On the distal side, less labeling was visible and syd localized to larger, often multivesicular organelles (Fig. 3 C). Quantification indicated clear accumulation of syd in the anterograde pool of transport vesicles as well as accumulation to a lesser extent in the retrograde pool (Fig. 3 D). In addition, we observed that the percentage of the membrane-bound syd labeling (i.e., gold particles within a distance of 15 nm or less from the closest membrane profile) is increased from 51.4% in the unligated nerve to 92.9% and 85.3% in the proximal and distal sides, respectively (Table I). Together these results indicate that syd is transported on axonal vesicles and that these vesicles travel in both directions.

Syd interacts with the dynactin complex

The observation of a retrograde pool of syd raised the possibility that syd interacts with the dynein/dynactin retrograde motor system. Coimmunoprecipitation experiments from sciatic nerve extracts showed that syd interacts with dynamitin (p50) and p150^{Glued}, two subunits of the dynactin complex (Fig. 4, A and B). Syd also interacts with kinesin light chain (KLC; Fig. 4 B), as shown previously (Bowman et al., 2000). We did not observe interaction between KLC or kinesin heavy chain (KIF5C) and p50 or p150^{Glued}, suggesting that syd binds either kinesin or dynactin, but not both simultaneously.

To further test the syd–dynactin interaction, we performed high resolution imaging of single axons. We observed significant colocalization between syd and p150^{Glued} in axons, stained with the neurofilament marker SMI31 (Fig. 4 C). A complete overlap was not expected because the coimmunoprecipitation experiment suggests that only a fraction of syd interacts with dynactin. Although no binding was detected between syd and the dynein intermediate chain (DIC; Fig. 4 A; Bowman et al., 2000), colocalization of syd with DIC was observed in transfected CV-1 cells (Bowman et al., 2000). Similarly, we observed partial colocalization between syd and the dynein heavy chain (DHC; Fig. 4 D). The extent of colocalization between syd and DHC is smaller than the one observed between syd and p150^{Glued}. This might account for the failure of syd antibodies to coimmunoprecipitate dynein. Similar results were found when the portions proximal and distal to a ligation were examined. These results suggest that membrane-bound syd interacts with the dynactin complex and perhaps indirectly with the dynein motor.

JNK is activated locally by sciatic nerve injury, primarily within axons

Previously, peripheral nerve transection in rat was shown to induce JNK activation in neuronal cell bodies (Kenney and Kocsis, 1998). To confirm that mouse sciatic nerve injury provoked by ligation also induces activation of JNK in neuronal cell bodies, we dissected and analyzed extracts of dorsal root ganglia (DRGs), which are enriched for sensory neuron cell bodies, 3, 6, and 8 h after sciatic nerve ligation. We observed an ~1.6-fold increase in the level of P-JNK on the ligated side compared with the contralateral unligated side at the 6 and 8 h time points, whereas no increase was detected at the 3-h time point. The levels of JNK1 and JNK3 were unchanged (Fig. 5 A). Similarly to syd and JNK3, P-JNK accumulates on both proximal and distal sides of the ligature, whereas only very faint staining was observed in the unligated nerve (Fig. 5 B). To assess directly whether or not the amount of activated JNK also increased locally upon nerve injury, sciatic nerves were ligated for 6 h, and the amount of P-JNK and JNK3 detected in ligated versus unligated nerves were compared biochemically (Fig. 5 C). Although the amount of P-JNK is increased in the ligated nerve, the levels of JNK1 and JNK3 remain constant (tubulin is used as a loading control). Sham surgery controls indicate that the increase in P-JNK is due to axonal injury induced by ligation rather than the surgery procedure. We measured the ratio between P-JNK and JNK3 at 1, 3, and 6 h after ligation (normalized to 1 in the unli-

gated nerve). We observed a threefold increase after 1 h of ligation (Fig. 5 D), with no further significant increase after 3 or 6 h. It is striking that the increase in P-JNK does not appear in the DRGs until the 6-h time point, whereas we observed an increase in P-JNK levels locally in the sciatic nerve after 1 h of ligation. This delay suggests that a retrogradely transported signal is mediating JNK activation in the cell bodies and might depend on local JNK activation. With an estimated retrograde transport velocity of $\sim 2 \mu\text{m/s}$, a molecule traveling from the injury site would require ~ 4 h to reach the DRGs, located ~ 3 cm away. Our results are in agreement with previous observations (Kenney and Kocsis, 1998), where the delay observed between axotomy and JNK activation in the DRGs corresponds to a signal transmission velocity in the 2 to 5- $\mu\text{m/s}$ range.

The sciatic nerve is enriched for axons but also contains the cell bodies of Schwann cells. Rat peripheral nerve transection was shown previously to increase P-JNK levels in the proximal stump (Sheu et al., 2000). However, this did not address whether JNK activation occurs within axons or in Schwann cells. To confirm that activation of JNK occurs locally in axons, we examined the distribution of JNK3 and P-JNK in sciatic nerve cross sec-

tions, $\sim 200 \mu\text{m}$ proximal and distal from the ligation site. JNK3 is present in axons and in some Schwann cells in unligated nerves and in both proximal and distal sides of ligated nerves (unpublished data). P-JNK staining is very faint in unligated nerves and is present mainly in axons of ligated sciatic nerves, with some Schwann cells also labeled (Fig. 5 E).

To test if activated JNK is associated with membranes in sciatic nerve, we prepared soluble (Fig. 5 F, S) and membrane-enriched fractions (Fig. 5 F, P) from unligated and ligated sciatic nerves. We observed that the ratio of PJNK/JNK3 increased by fourfold in the soluble pool and by threefold in the membrane pool (Fig. 5 F). These results indicate that JNK is activated locally, mainly within axons, following nerve injury, in addition to the activation observed in the cell body, and that a fraction of P-JNK is present on membranes.

Activated JNK and *syd* are transported retrogradely following injury

Typical single sciatic nerve ligation experiments indicated that *syd* and JNK3 are transported predominantly in the anterograde direction (Fig. 3) and that the injury caused by the ligation

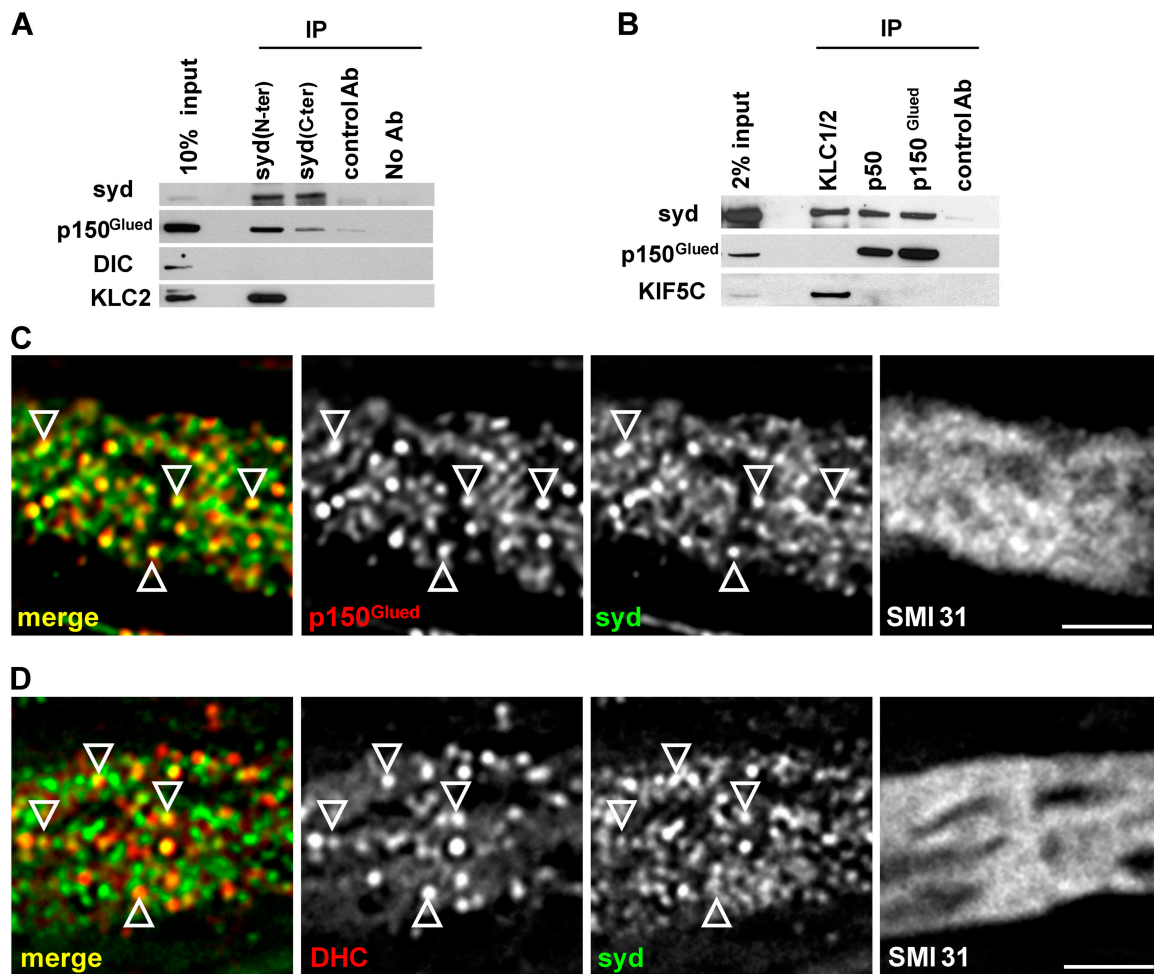


Figure 4. **Syd interacts with the dynactin complex.** (A and B) Coimmunoprecipitation from sciatic nerve extract was probed with the indicated antibodies. A subunit of the dynactin complex, p150^{Glued}, coimmunoprecipitates with *syd*. The reverse experiment shows coimmunoprecipitation of *syd* with KLC, p50, and p150^{Glued}. (C and D) Deconvoluted images of sciatic nerve longitudinal sections show partial colocalization (arrowheads) between *syd* and p150^{Glued} and between *syd* and DHC within a single axon (stained with the neurofilament marker SMI31). Bars, 2 μm .

leads to local axonal JNK activation. Previous workers (Kenney and Kocsis, 1998) reported the appearance of P-JNK in neuronal cell bodies in a time- and distance-dependent manner from the injury site, suggesting the existence of a microtubule-dependent signaling system. To test if P-JNK itself is a positive injury signal and travels retrogradely toward the cell body after injury, we performed a double ligation experiment (i.e., two ligatures were placed 8 mm apart). This design allowed us to examine transport in an injured nerve segment without contributions of new material transported from the cell body or from the nerve terminal. In this design, the proximal ligation represents a collecting site for molecules traveling from the distal ligation. After 6 h, the nerve was dissected and divided into two equal parts representing retrograde (Fig. 6 B, R) and anterograde (Fig. 6 B, A) fractions (Fig. 6 B, scheme). P-JNK, JNK3, and syd were enriched in the retrograde pool, whereas APP was

enriched in the anterograde pool (Fig. 6, A and B). A similar observation was made when the portions corresponding to the retrograde and anterograde pool close to the ligation sites were examined by immunofluorescence (Fig. 6 C). These results suggest that upon encountering an injury, anterograde syd and P-JNK switch to the retrograde pathway, whereas APP transport is not affected and remains mainly anterograde.

Because syd interacts with the dynactin complex and colocalizes in axons with p150^{Glued} and DHC (Fig. 4), this interaction could mediate axonal retrograde transport. To further support the suggestion that P-JNK retrograde transport after injury depends on syd and the dynactin–dynein motor complex, we examined the localization of P-JNK in axons distal to a ligation site. We observed that P-JNK colocalized with both p150^{Glued} and DHC (Fig. 7, A and B). Consistent with what we observed for syd, the extent of colocalization is higher with

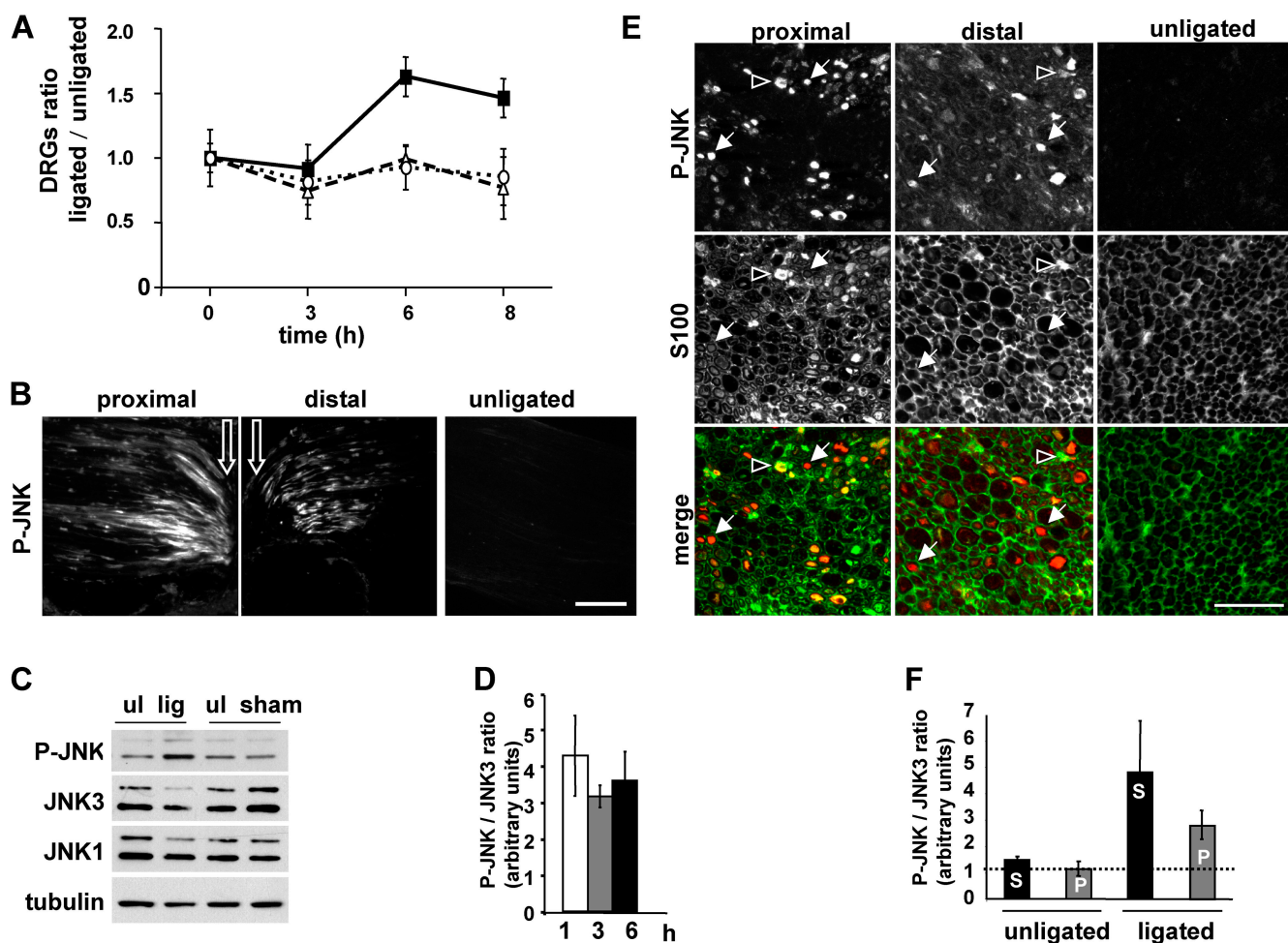


Figure 5. JNK is activated locally by sciatic nerve injury. (A) Sciatic nerve ligation was performed as in Fig. 3. Mice were killed 3, 6, or 8 h after surgery. DRGs on the ligated and contralateral unligated sides were dissected and analyzed by SDS-PAGE. Levels of P-JNK (closed squares), JNK1 (open circles), and JNK3 (open triangles) were normalized to tubulin, and the ratios between ligated and unligated were measured. Results represent mean \pm SEM ($n = 4$). (B) Sciatic nerves were ligated unilaterally at the midpoint and stained for P-JNK. White arrows show ligation site. (C) Whole ligated nerve (lig), sham operated nerve (sham), and contralateral unligated (ul) nerve were dissected and homogenized, and extracts were analyzed by SDS-PAGE and Western blot (Western blot is representative of seven independent experiments; only the 6-h time point is shown). (D) Quantification of the relative ratio P-JNK/JNK3 between ligated and unligated nerves is shown \pm SEM ($n = 7$). The P-JNK/JNK3 ratio in unligated nerve was normalized to 1. The level of P-JNK increased threefold in the ligated nerves after 1, 3, and 6 h. (E) Sciatic nerve cross sections $\sim 200 \mu\text{m}$ proximal or distal of the ligation site were stained for P-JNK and S100. Arrows, P-JNK staining in axon; arrowheads, P-JNK staining in Schwann cells. (F) Ligated and unligated nerves were subjected to high speed centrifugation. Soluble (S) and membrane-bound fractions (P) were analyzed by Western blot. The ratio P-JNK/JNK3 was determined as in B and shown as mean \pm SEM ($n = 4$). Bars: (B) $100 \mu\text{m}$; (E) $20 \mu\text{m}$.

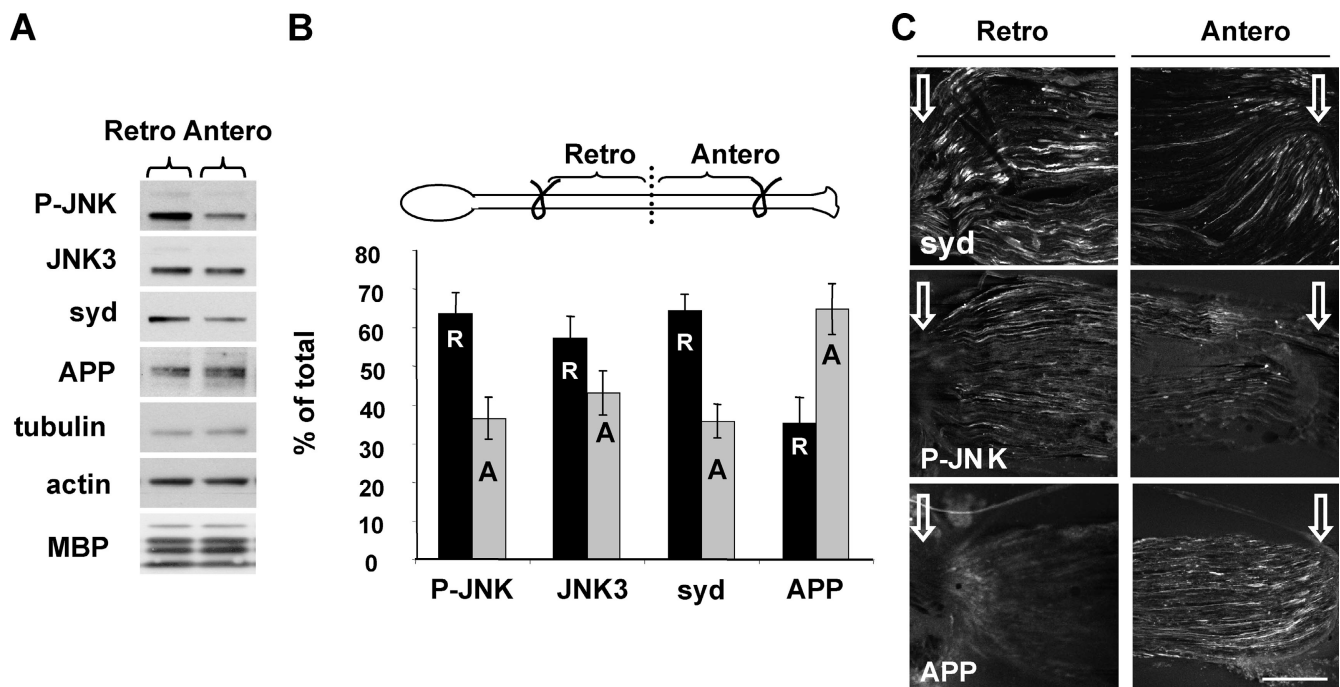


Figure 6. P-JNK and syd are transported mainly retrogradely after nerve injury. (A) Sciatic nerve double ligation was performed with 2 knots 8 mm apart for 6 h (B, scheme). The nerve was dissected, divided into two equal parts representing the retrograde (Retro) and anterograde (Antero) pool, and analyzed by SDS-PAGE. Replicates are shown in the online supplemental material. (B) Quantification of the fraction of retrograde (R, black bars) and anterograde (A, gray bars) over total (A + R) (\pm SEM; $n = 5$). (C) Values were normalized to the level of tubulin as in A, but the retrograde and anterograde pools were analyzed by immunofluorescence. The ligation site is indicated with white arrows. Bar, 100 μ m.

p150^{Glued} than with DHC. P-JNK and syd were also found to colocalize on the same puncta (Fig. 7 C). Similar results were found when the portion proximal to the ligation site was analyzed (unpublished data).

Sciatic nerve injury induces an increase in syd/dynactin association

Although generally increased axonal transport following injury has been demonstrated (Curtis et al., 1998), evidence for injury-induced transport of signaling molecules other than neurotrophins does not exist (Delcroix et al., 2003a). Thus, we tested if sciatic nerve injury results in an increase of syd association with the dynactin complex, which might account for a switch to retrograde transport. By performing sucrose density sedimentation analysis, we observed that the soluble pool of syd is found exclusively at \sim 8S (unpublished data), whereas the membrane-associated pool is found in two peaks, \sim 8S and \sim 17S. To test if the syd peak at \sim 17S reports an interaction with dynactin, we performed sucrose density gradient sedimentation analysis following dynactin immunodepletion. p150^{Glued} and p50 were immunodepleted from membrane extract of injured and noninjured sciatic nerves; the resulting extract was analyzed by sucrose density sedimentation. The amount of syd, p150^{Glued}, DIC, and KIF5C is constant in extracts prepared from unligated or ligated nerves (Fig. 8 A). In contrast, P-JNK levels are higher in the ligated nerves, as expected. Tubulin and myelin basic protein serve as loading controls. The efficiency of the immunodepletion showed that most of the p150^{Glued} is removed on the antibody-coated beads because none can be detected in the gradient fractions, in contrast to the mock deple-

tion with GFP antibodies (Fig. 8, A and B). No difference was observed in the sedimentation properties of DIC and KIF5C in both ligated and unligated nerves in the presence or absence of the dynactin subunits p50 and p150^{Glued}. DIC peaked at \sim 18–19S, whereas KIF5C peaked at \sim 4–11S as expected (Kamal et al., 2000). Syd distribution is characterized by two main peaks, one at \sim 8S and one at \sim 17S, indicating that syd exists at least in two protein complexes of distinct composition. In sciatic nerves injured by ligation, the amount of membrane-associated syd increased in the \sim 17S fraction and decreased in the \sim 8S fraction compared with the unligated situation (Fig. 8 B, top; and Fig. S2 C). The P-JNK distribution across the sucrose gradients was restricted to the low density fractions (unpublished data; the interaction between P-JNK and dynactin might be weak as reflected by the low amount detected in the dynactin immunoprecipitation). After dynactin depletion, the syd injury-induced increase at \sim 17S is lost and a resulting increase at 4–8S is observed. These results suggest that membrane-associated syd exists in several complexes of different sedimentation properties. In uninjured nerves, the syd complex sedimenting at 17S does not reflect dynactin association. However, the increased population of syd at 17S following injury appears to require interaction with the dynactin complex and can account for the observed injury-induced retrograde transport of syd.

Discussion

The ability of neurons to regenerate axons following injury relies on alterations of gene transcription, but little is known about how information from the site of injury is communicated to the

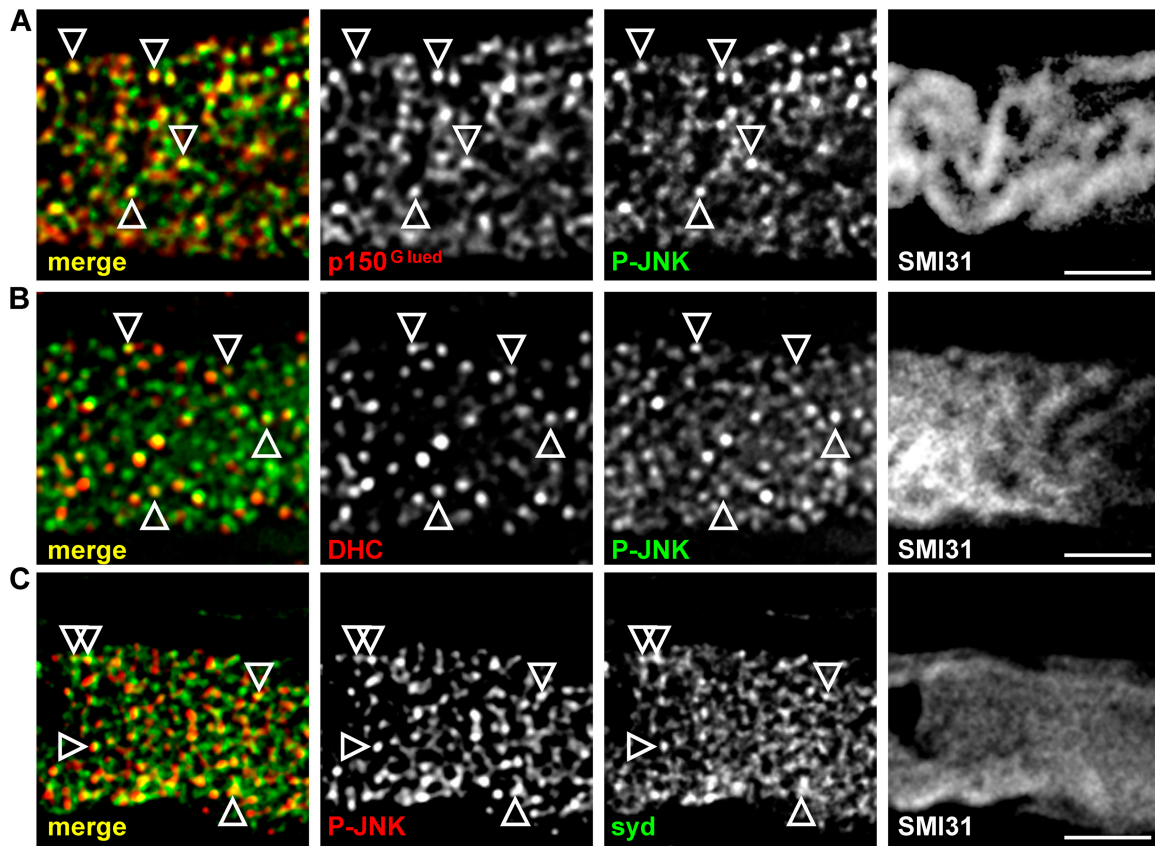


Figure 7. **P-JNK colocalizes with dynactin, dynein, and syd in axons distal to a ligation.** (A–C) Deconvoluted images of single axons, stained with SMI31 and the indicated antibodies, distal to the ligation site. Arrowheads show colocalized puncta. Bars, 2 μ m.

cell body to initiate these changes. This is a challenging problem because the site of lesion is often distant from the cell body and the response must be rapid and persist for weeks until axon regeneration is completed. Our data suggest that part of the solution to this problem is that axonal JNK is activated locally as part of a retrograde axonal damage signal and that syd may mediate both the anterograde and retrograde transport of JNK via interaction with kinesin-I and dynactin/dynein, respectively.

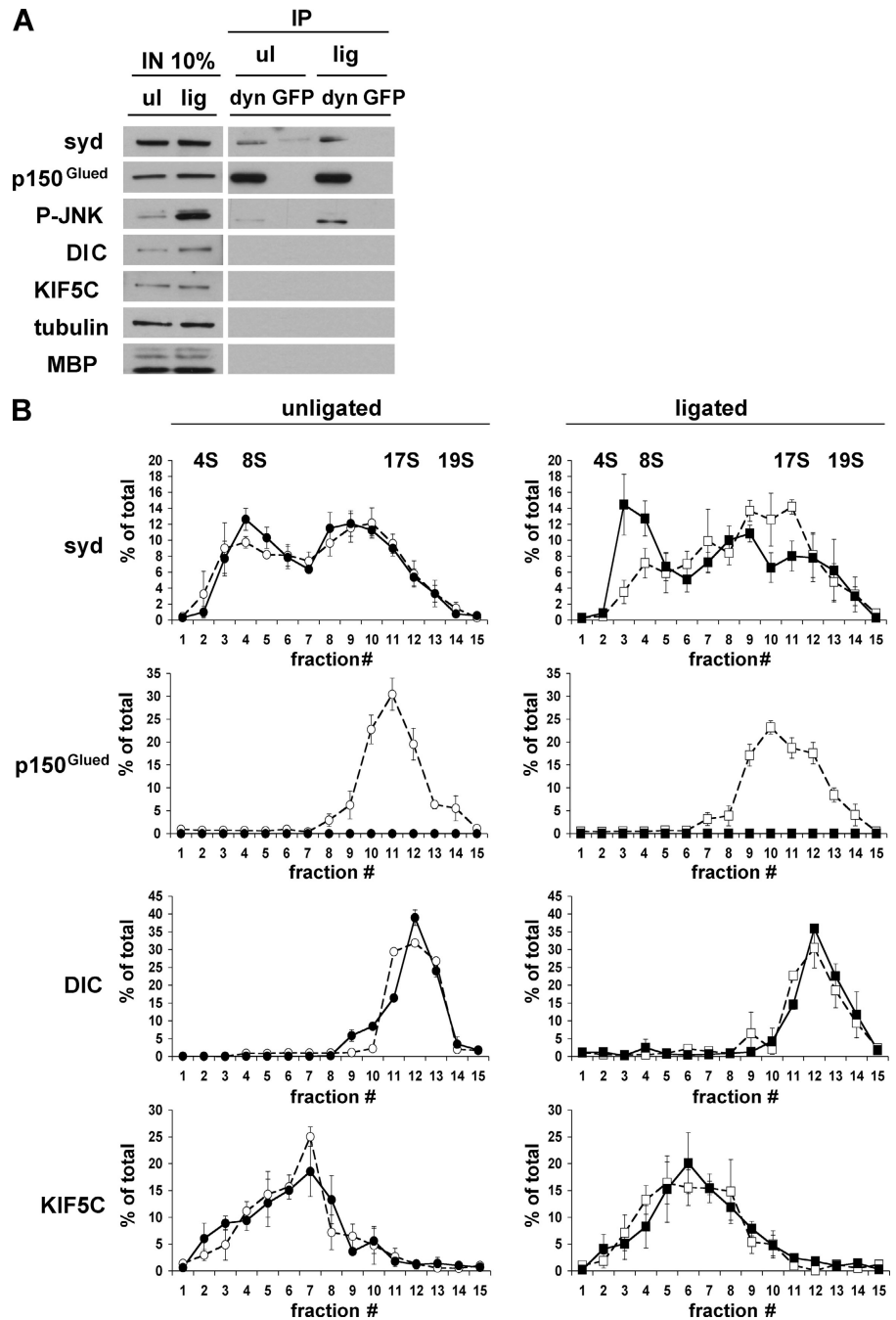
Our proposal is consistent with other work suggesting that the axonal transport machinery may not only convey structural components and organelles but also molecules used to transmit information about distant events between the nerve terminal and the cell body. For example, a subset of the signaling components in the MAPK pathway, including PI3K, ERK1/2, p38MAPK, and JNK, are transported along axons (Johanson et al., 1995; Middlemas et al., 2003). In this regard, JNK scaffolding proteins have been proposed to target JNK kinases to specific subcellular locations. The finding that three members of the JNK scaffolding protein family, JIP1, JIP2, and syd, interact with kinesin-I conforms to the proposal that JNK signal reception or transmission is in part mediated by microtubule-based transport of a JNK–JIP complex (Bowman et al., 2000; Verhey et al., 2001). Also consistent with this view is the observed concentration of the three JNK scaffolding proteins in process termini of cultured central nervous system catecholaminergic cells, which requires kinesin (Verhey et al., 2001). Similarly, it was reported that in cultured hippocampal neurons exposed to

anoxic stress, JIP1 is redistributed from neurites to the perinuclear region (Whitmarsh et al., 2001). The *Caenorhabditis elegans* orthologue of syd, UNC-16, is proposed to regulate the localization of vesicular cargo by integrating JNK signaling and kinesin-1 transport (Byrd et al., 2001), although in PC12 cells, JSAP1/syd transport to the growth cone of neurites is apparently independent of JNK signaling (Sato et al., 2004). Our finding that JNK is activated at injury sites within axons and that activated JNK and syd then travel mainly retrogradely following injury supports the hypothesis that JNK and syd in axons might establish a damage surveillance mechanism.

Posttranslational modifications occurring after injury might affect syd binding affinity for kinesin and trigger binding to the dynactin complex and recruitment to membranes. Our finding that after nerve injury a high molecular weight complex of membrane-associated syd is associated with dynactin is in agreement with this hypothesis. In addition, upon JNK activation, syd is phosphorylated on threonine and serine residues (Ito et al., 1999; Kelkar et al., 2000). In this regard, syd and dynactin may be part of the coordination machinery regulating anterograde and retrograde transport (Gross et al., 2002; Deacon et al., 2003)

If activated JNK is transported from the injury site back to the cell body, there must be mechanisms that ensure a persistent active state. In the case of NGF signaling, NGF binds and activates TrkA, and the complex then moves retrogradely in association with a signaling endosome (Delcroix et al., 2003b).

Figure 8. Syd association with the dynactin complex is increased by injury. The dynactin complex was immunodepleted from membrane-bound material of ligated or unligated sciatic nerves. For dynactin depletion, both p150^{Glued} and p50 antibodies were used, whereas for mock depletion a GFP antibody was used. (A) SDS-PAGE analysis of immunodepletion using dynactin (dyn) or GFP antibodies. Note that input (IN) and immunoprecipitated material (IP) are from equivalent exposures, except for blots with syd and P-JNK antibodies, which required higher exposure times. (B) The unbound (nonimmunoprecipitated) material was sedimented on 5–20% linear sucrose gradients. Fractions were resolved by SDS-PAGE and Western blots were performed using syd, p150^{Glued}, DIC, and KIF5C antibodies. Quantification is expressed as a percentage of total \pm SEM ($n = 3$). Dynactin depletion (closed symbols) and mock GFP depletion (open symbols) is shown. A representative Western blot is shown in the online supplemental material.



This retrograde movement may be due to an interaction between activated Trk and dynein (Yano et al., 2001; Bhattacharyya et al., 2002). Recent data suggest that the specialized NGF/TrkA endosome has persistent signaling potential (Shao et al., 2002). The upstream MAPKKs MLK3 and MEK1 and the MAPKKs SEK1/MKK4 and MKK7 may also bind syd (Nagata et al., 1998; Ito et al., 1999; Kelkar et al., 2000) and might be transported together with JNK to ensure prolonged activation of JNK during retrograde transport. Such a JNK “signalsome” might travel along microtubules for active signaling from distant locations. Other scaffolding proteins might also participate in the retrograde transport of JNK. β -Arrestin-2, in addition to its role in endocytosis and G-coupled re-

ceptor desensitization, is another scaffold for JNK3 (McDonald et al., 2000). β -Arrestin-2 contains a nuclear export signal and mediates JNK3 nuclear localization in appropriate conditions (Scott et al., 2002). Activated JNK3 has a greater affinity for β -arrestin-2 than the nonactivated form, and the possibility that β -arrestin-2 plays a role in the retrograde transport of JNK and nuclear translocation awaits further investigation.

The identities of the signals that inform the cell body that the axon has been injured are still obscure. Multiple signals functioning in a temporal sequence seem to be involved (for review see Ambron and Walters, 1996). First, action potentials propagating from the injury site to the cell body may activate a kinase cascade in the cell soma. Second are the so-called nega-

tive injury signals, in which axotomy prevents molecules that are normally transported retrogradely from reaching the cell body. Third, positive injury signals may be activated at the injury site and transported retrogradely back to the cell body. The targets of positive signals include transcription factors that exert control over synthesis of proteins necessary for regeneration (Sung et al., 2001). There is now accumulating evidence indicating that the transcription factors themselves can act as positive injury signals. Studies in the *Aplysia* mollusc have shown that NLS can target retrograde transport and nuclear uptake of heterologous proteins (Schmied and Ambron, 1997). Although it was recently shown that protein kinase G (ApPKG) is activated at injury sites and retrogradely transported (Sung et al., 2004), the mechanism responsible for injury-induced transport is still unknown. The transcription factors ATF2 and NF- κ -B are transported in axons (Delcroix et al., 1999; Wellmann et al., 2001). Recently, the signal transducer and activator of transcription STAT3 has been found to be activated in injured axons and is proposed to play a role as a retrograde signal transcription factor (Lee et al., 2004). The proinflammatory cytokine tumor necrosis factor- α also increases at the injury site and undergoes retrograde axonal transport (Shubayev and Myers, 2001).

Another class of positive injury signals now seems to include axonal mRNA. It was shown recently that after nerve injury β -importin protein levels are increased by local translation of axonal mRNA, leading to the formation of an NLS binding complex traveling retrogradely (Hanz et al., 2003). The list of positive injury signals will increase, and approaches like differential proteomics will be of great help in revealing retrogradely transported components after nerve injury (Perlson et al., 2004).

The observation that JNK activation following axotomy persists until target reinnervation has occurred indicates a positive role for JNK signaling in neuronal survival and repair in addition to the immediate injury response (Kenney and Kocsis, 1998). In fact, several classes of positive injury signals may coexist to ensure precise information on the nature of the damage and its distance from the cell body. For example, activation of JNK along the length of the axon has been reported previously in a mouse model of type-I diabetes, probably as a result of hyperglycemic stress of the peripheral nerve, and may represent a retrograde signaling system for nerve degeneration (Middlemas et al., 2003). However, in the case of mechanical damage occurring upon nerve injury, a retrograde signal involving JNK may support nerve survival and regeneration (Kenney and Kocsis, 1998). Therefore, the upstream cascade leading to JNK activation might be relevant for neuronal survival or death. Studies in *Aplysia* have shown that axotomy triggers short- and long-term activation of an Elk1-SRF transcription complex in response to electrical signals and axoplasmic Elk1 retrograde transport, respectively (Lin et al., 2003). Thus, coordination between several injury signals might orchestrate the precise program ensuring nerve regeneration or degeneration.

In addition to a role in transcription factor activation in the cell body, JNK may have downstream axoplasmic substrates and play an active role in neurite outgrowth. Indeed the recent finding that JNK may phosphorylate neuronal microtubule-associated proteins supports this possibility (Chang et al., 2003).

Materials and methods

Antibodies

Syd antibodies were obtained by immunizing rabbits with the recombinant fragments 6 \times HIStag residues 1–772 (syd NH₂-terminal) and 6 \times HIStag residues 1066–1328 (syd COOH-terminal; Bowman et al., 2000). For some experiments, syd antibodies were conjugated to Alexa-488 or to protein A-sepharose according to the manufacturer's instructions (Molecular Probes; Pierce Chemical Co.). The following antibodies were used: anti-JIP3 (a gift from R.J. Davis, University of Massachusetts, Worcester, MA), anti-DHC (a gift from P. Grissom and J.R. McIntosh, University of Colorado, Boulder, CO), anti-p150^{GluEd} (a gift from E. Holzbaur, University of Pennsylvania, Philadelphia, PA), anti-p150^{GluEd} and anti-p50 (BD Biosciences), anti-JNK1 and anti-JNK2 (BD Biosciences), anti-JNK3 (Upstate Biotechnology), anti-P-JNK and anti-P-TrkA (Cell Signaling), anti-S100 and antitubulin DM1A (Sigma-Aldrich), anti-KLC1/2 (a gift from S. Brady, University of Illinois, Chicago, IL), anti-DIC and anti-APP (Chemicon), anti-syntaxin 13 (Synaptic Systems GmbH), anti-myelin basic protein (DakoCytomation), anti-syntaxin (StressGen Biotechnologies), anti-KIF5C (prepared by C.H. Xia, University of California, Berkeley, Berkeley, CA; Xia et al., 2003), anti-COX1 and secondary Alexa-labeled antibodies (Molecular Probes), and anti-EEA1 (Transduction Laboratories).

Biochemical characterization of syd

For flotation experiments, mouse brain or sciatic nerve was homogenized in homogenization buffer (8% sucrose and 3 mM imidazole, pH 7.4). A postnuclear supernatant (PNS) was prepared and loaded at the bottom of a sucrose step gradient. After centrifugation at 100,000 g for 2 h at 4°C, floating fractions were collected and equal amounts of proteins were analyzed by SDS-PAGE and Western blot.

Triton X-114 phase separation was performed as previously described (Bordier, 1981). In brief, sciatic nerve extracts were incubated with Triton X-114 at 4°C for 1 h, centrifuged 5 min at 4°C at 10,000 g, loaded over a 6% sucrose cushion, incubated 3 min at 30°C, and centrifuged 5 min at 10,000 g. Equal proportions of detergent and aqueous phases were analyzed by SDS-PAGE and Western blot. To release peripheral membrane proteins, sciatic nerve PNS was incubated twice at 4°C for 30 min in 0.1 M Na₂CO₃ and centrifuged 1 h at 100,000 g. Equal proportions of supernatant and pellet were analyzed. For trypsin digestion, a brain membrane fraction was prepared by step sucrose gradient, incubated 30 min at 4°C with the indicated amount of trypsin (microgram of trypsin/microgram of total protein), with or without soybean trypsin inhibitor and Triton X-100, and analyzed by SDS-PAGE with the indicated antibodies.

For sucrose density gradients, eight ligated and contralateral unligated sciatic nerves were homogenized in buffer A (50 mM Tris, 150 mM NaCl, pH 7.4, and 0.5 mM EDTA) plus protease inhibitors and centrifuged sequentially 10 min at 1,000 g, 10 min at 10,000 g, and 50 min at 100,000 g. The high speed pellet was resuspended in buffer A + 1% Triton X-100. Dynactin was immunodepleted and the supernatant was overlaid onto a continuous 5–20% sucrose gradient prepared in buffer A and centrifuged at 35,000 g for 17 h in a rotor (model SW41; Beckman Coulter). 0.5-ml fractions were collected and analyzed by SDS-PAGE and Western blot. Gradients loaded with the markers carbonic anhydrase, BSA, alcohol dehydrogenase, β -amylase, catalase, apoferritin, and thyroglobulin were run in parallel as standards to determine 2.8S, 4.2S, 7.5S, 9S, 11S, 17S, and 19S, respectively.

Protein concentration was determined using the protein assay (Bio-Rad Laboratories). For quantification of Western blots, ECL signals in the linear range were scanned using NIH image 1.62.

Immunoprecipitation

Sciatic nerve PNS was diluted in lysis buffer (150 mM NaCl, 25 mM Tris-HCl, pH 7.5, 1 mM EDTA, 1 mM EGTA, 1% Triton X-100, 2.5 mM sodium pyrophosphate, 1 mM β -glycerophosphate, 1 mM Na₃VO₄, and protease inhibitors). Extracts were incubated with the indicated antibodies or with GFP antibody as a control for 3 h at 4°C followed by incubation with 0.5% BSA-coated protein A- or G-sepharose for 1 h at 4°C. Beads were washed five times with PBS, resuspended in sample buffer, and analyzed by SDS-PAGE and Western blot.

Sciatic nerve ligation

Sciatic nerve ligation experiments were done as described previously (Kamal et al., 2000) with minor modifications. In brief, the sciatic nerves of mice were ligated unilaterally at the midpoint, and mice were killed at the indicated time after surgery. To avoid contamination of proximal and dis-

tal parts, two ligations were placed 1 mm apart. For sham-operated controls, the sciatic nerve was exposed by surgery but the ligature was omitted. For biochemistry, equal lengths of the proximal and distal parts were homogenized in sample buffer and equal volumes were loaded and analyzed by SDS-PAGE and Western blotting. The tubulin Western blot serves as a loading control. Double ligation experiments were performed by exposing the sciatic nerve over a 1-cm length at mid-thigh level. Two knots were placed 8 mm apart. Equal lengths corresponding to the anterograde or retrograde pool were homogenized in sample buffer, and equal amounts of protein were loaded and analyzed by SDS-PAGE. For DRGs analysis following ligation, L4, L5, and L6 DRGs were dissected, homogenized in sample buffer, and analyzed by SDS-PAGE. All surgeries were performed using adult female C57/bl6 mice anesthetized with isoflurane. All procedures were approved by the University of California, San Diego, animal welfare program.

Immunofluorescence

Sciatic nerves were dissected and post-fixed 2 h in 3.7% PFA in PBS. Nerves were incubated overnight in 20% sucrose, embedded in Histo Prep, and frozen in dry-ice-cooled methanol. Serial 10- μ m cryostat sections were cut and mounted onto coated slides (Fisher Scientific). Sections were permeabilized and blocked with 10% goat serum, 0.1% Triton X-100 in PBS for 30 min. Sections were incubated with the indicated primary antibodies overnight at 4°C and with Alexa-conjugated secondary antibodies for 3 h. For high resolution images, sections were observed with a 100 \times objective on a deconvolving microscope (Delta Vision). Images of 0.15- μ m optical sections were acquired in SoftWoRx software (Applied Precision Inc.). Several (20–30) optical sections were deconvoluted for each experiment using the SoftWoRx program, and a single deconvoluted optical section is shown in each figure. For low resolution images, sections were observed with a 20 or 63 \times objective on a confocal microscope (model MRC1024; Bio-Rad Laboratories).

EM

Sciatic nerves were prepared for ultrathin cryosectioning and immunogold labeling according to the protein A gold method as described previously (Slot et al., 1991). In brief, sciatic nerves were dissected and fixed in a mixture of 2% PFA and 0.2% glutaraldehyde in 0.1 M phosphate buffer for 2 h at RT, and then over night at 4°C, and stored in 1% PFA in phosphate buffer at 4°C, after which they were washed in PBS with 0.02 M glycine. After overnight infiltration with 2.3 M sucrose at 4°C, the desired nerve regions were mounted on specimen holders and frozen in liquid nitrogen. Ultrathin cryosections with an average thickness of 60 nm were cut with a diamond knife (Diatome) at –120°C and were picked up in a 1:1 mixture of 2.3 M sucrose and 2% methyl cellulose in distilled water. The sections were thawed to RT, incubated with syd NH₂-terminal antibodies and 15 nm of protein A gold, contrasted and embedded with 0.4% uranylacetate in 2% methyl cellulose, and viewed under a transmission electron microscope (model 1200 EX; JEOL). For quantification analysis, total gold particles were counted on an area of 100 μ m² on both proximal and distal axoplasm and an equivalent area on an unligated nerve axoplasm. As a negative control, sections were treated only with 15 nm of protein A gold to indicate unspecific labeling in each case.

Online supplemental material

Online supplemental material describes the characterization of syd antibodies and shows representative Western blots for sciatic nerve ligation experiments. Online supplemental material is available at <http://www.jcb.org/cgi/content/full/jcb.200410136/DC1>.

We thank R.J. Davis for the anti-JIP3 antibody; E. Holzbaur for anti-p150^{Glued} polyclonal antibody; P.M. Grissom and J.R. McIntosh for anti-DHC antibody; Brendan Brinkman for expert technical assistance with the Delta Vision deconvolution microscope; Eileen Westerman for expert technical assistance with anesthesia; Giampietro Schiavo for helpful discussions; and Peter van der Sluijs, Angels Almenar-Queralt, and Kristina Schimmelpfeng for critical reading of the manuscript.

L.S.B. Goldstein is an investigator of the Howard Hughes Medical Institute. V. Cavalli was supported by postdoctoral fellowships from the Christopher Reeve Paralysis Foundation and the Swiss National Science Foundation. P. Kujala was supported by grant ALW8PJ/00-31 from the Research Council for Earth and Life Sciences (Nederlandse Organisatie voor Wetenschappelijk Onderzoek–Aard- en LevensWetenschappen) that was assigned to J. Klumperman.

Submitted: 28 October 2004

Accepted: 6 January 2005

References

- Ambron, R.T., and E.T. Walters. 1996. Priming events and retrograde injury signals. A new perspective on the cellular and molecular biology of nerve regeneration. *Mol. Neurobiol.* 13:61–79.
- Bhattacharyya, A., F.L. Watson, S.L. Pomeroy, Y.Z. Zhang, C.D. Stiles, and R.A. Segal. 2002. High-resolution imaging demonstrates dynein-based vesicular transport of activated Trk receptors. *J. Neurobiol.* 51:302–312.
- Bordier, C. 1981. Phase separation of integral membrane proteins in Triton X-114 solution. *J. Biol. Chem.* 256:1604–1607.
- Bowman, A.B., A. Kamal, B.W. Richtigings, A. Philp, M. McGrail, J.G. Gindhardt, and L.S.B. Goldstein. 2000. Kinesin-dependent axonal transport is mediated by the sunday driver (SYD) protein. *Cell.* 103:583–594.
- Byrd, D.T., M. Kawasaki, M. Walcoff, N. Hisamoto, K. Matsumoto, and Y. Jin. 2001. UNC-16, a JNK-signaling scaffold protein, regulates vesicle transport in *C. elegans*. *Neuron.* 32:787–800.
- Chang, L., Y. Jones, M.H. Ellisman, L.S. Goldstein, and M. Karin. 2003. JNK1 is required for maintenance of neuronal microtubules and controls phosphorylation of microtubule-associated proteins. *Dev. Cell.* 4:521–533.
- Curtis, R., J.R. Tonra, J.L. Stark, K.M. Adryan, J.S. Park, K.D. Cliffer, R.M. Lindsay, and P.S. DiStefano. 1998. Neuronal injury increases retrograde axonal transport of the neurotrophins to spinal sensory neurons and motor neurons via multiple receptor mechanisms. *Mol. Cell. Neurosci.* 12:105–118.
- Davis, R.J. 2000. Signal transduction by the JNK group of MAP kinases. *Cell.* 103:239–252.
- Deacon, S.W., A.S. Serpinskaya, P.S. Vaughan, M. Lopez Fanarraga, I. Vernos, K.T. Vaughan, and V.I. Gelfand. 2003. Dynactin is required for bidirectional organelle transport. *J. Cell Biol.* 160:297–301.
- Delcroix, J.D., S. Averill, K. Fernandes, D.R. Tomlinson, J.V. Priestley, and P. Fernyhough. 1999. Axonal transport of activating transcription factor-2 is modulated by nerve growth factor in nociceptive neurons. *J. Neurosci.* 19:RC24.
- Delcroix, J.D., J. Patel, S. Averill, D.R. Tomlinson, J.V. Priestley, and P. Fernyhough. 2003a. Peripheral axon crush elevates transport of p75NTR in the central projection of sensory neurones of rats. *Neurosci. Lett.* 351:181–185.
- Delcroix, J.D., J.S. Valletta, C. Wu, S.J. Hunt, A.S. Kowal, and W.C. Mobley. 2003b. NGF signaling in sensory neurons: evidence that early endosomes carry NGF retrograde signals. *Neuron.* 39:69–84.
- Ehlers, M.D., D.R. Kaplan, D.L. Price, and V.E. Koliatsos. 1995. NGF-stimulated retrograde transport of trkA in the mammalian nervous system. *J. Cell Biol.* 130:149–156.
- Gross, S.P., M.A. Welte, S.M. Block, and E.F. Wieschaus. 2002. Coordination of opposite-polarity microtubule motors. *J. Cell Biol.* 156:715–724.
- Hanz, S., E. Perlson, D. Willis, J.Q. Zheng, R. Massarwa, J.J. Huerta, M. Koltzenburg, M. Kohler, J. van-Minnen, J.L. Twiss, and M. Fainzilber. 2003. Axoplasmic importins enable retrograde injury signaling in lesioned nerve. *Neuron.* 40:1095–1104.
- Herdegen, T., P. Skene, and M. Bahr. 1997. The c-Jun transcription factor—bipotential mediator of neuronal death, survival and regeneration. *Trends Neurosci.* 20:227–231.
- Ito, M., K. Yoshioka, M. Akechi, S. Yamashita, N. Takamatsu, K. Sugiyama, M. Hibi, Y. Nakabeppu, T. Shiba, and K.I. Yamamoto. 1999. JSAP1, a novel jun N-terminal protein kinase (JNK)-binding protein that functions as a Scaffold factor in the JNK signaling pathway. *Mol. Cell. Biol.* 19:7539–7548.
- Jenkins, R., and S.P. Hunt. 1991. Long-term increase in the levels of c-jun mRNA and jun protein-like immunoreactivity in motor and sensory neurons following axon damage. *Neurosci. Lett.* 129:107–110.
- Johanson, S.O., M.F. Crouch, and I.A. Hendry. 1995. Retrograde axonal transport of signal transduction proteins in rat sciatic nerve. *Brain Res.* 690:55–63.
- Kamal, A., G.B. Stokin, Z. Yang, C. Xia, and L.S. Goldstein. 2000. Axonal transport of amyloid precursor protein is mediated by direct binding to the kinesin light chain subunit of kinesin-I. *Neuron.* 28:449–459.
- Karki, S., and E.L. Holzbaur. 1999. Cytoplasmic dynein and dynactin in cell division and intracellular transport. *Curr. Opin. Cell Biol.* 11:45–53.
- Kelkar, N., S. Gupta, M. Dickens, and R.J. Davis. 2000. Interaction of a mitogen-activated protein kinase signaling module with the neuronal protein JIP3. *Mol. Cell. Biol.* 20:1030–1043.
- Kenney, A.M., and J.D. Kocsis. 1998. Peripheral axotomy induces long-term c-Jun amino-terminal kinase-1 activation and activator protein-1 binding activity by c-Jun and junD in adult rat dorsal root ganglia *In vivo*. *J. Neurosci.* 18:1318–1328.
- Kuan, C.Y., D.D. Yang, D.R. Samanta Roy, R.J. Davis, P. Rakic, and R.A. Flavell. 1999. The Jnk1 and Jnk2 protein kinases are required for regional

- specific apoptosis during early brain development. *Neuron*. 22:667–676.
- Leah, J.D., T. Herdegen, and R. Bravo. 1991. Selective expression of Jun proteins following axotomy and axonal transport block in peripheral nerves in the rat: evidence for a role in the regeneration process. *Brain Res*. 566: 198–207.
- Lee, N., K.L. Neitzel, B.K. Devlin, and A.J. MacLennan. 2004. STAT3 phosphorylation in injured axons before sensory and motor neuron nuclei: potential role for STAT3 as a retrograde signaling transcription factor. *J. Comp. Neurol.* 474:535–545.
- Lin, H., J. Bao, S. Ying-Ju, E.T. Walters, and R.T. Ambron. 2003. Rapid electrical and delayed molecular signals regulate the serum response element after nerve injury: convergence of injury and learning signals. *J. Neurobiol.* 57:204–220.
- McDonald, P.H., C.W. Chow, W.E. Miller, S.A. Laporte, M.E. Field, F.T. Lin, R.J. Davis, and R.J. Lefkowitz. 2000. Beta-arrestin 2: a receptor-regulated MAPK scaffold for the activation of JNK3. *Science*. 290:1574–1577.
- Middlemas, A., J.D. Delcroix, N.M. Sayers, D.R. Tomlinson, and P. Fernyhough. 2003. Enhanced activation of axonally transported stress-activated protein kinases in peripheral nerve in diabetic neuropathy is prevented by neurotrophin-3. *Brain*. 126:1671–1682.
- Nagata, K., A. Puls, C. Futter, P. Aspenstrom, E. Schaefer, T. Nakata, N. Hirokawa, and A. Hall. 1998. The MAP kinase kinase kinase MLK2 colocalizes with activated JNK along microtubules and associates with kinesin superfamily motor KIF3. *EMBO J.* 17:149–158.
- Paschal, B.M., and R.B. Vallee. 1987. Retrograde transport by the microtubule-associated protein MAP 1C. *Nature*. 330:181–183.
- Pelerson, E., S. Hanz, K.F. Medzihradsky, A.L. Burlingame, and M. Fainzilber. 2004. From snails to sciatic nerve: Retrograde injury signaling from axon to soma in lesioned neurons. *J. Neurobiol.* 58:287–294.
- Raivich, G., M. Bohatschek, C. Da Costa, O. Iwata, M. Galiano, M. Hristova, A.S. Nateri, M. Makwana, L. Riera-Sans, D.P. Wolfner, et al. 2004. The AP-1 transcription factor c-Jun is required for efficient axonal regeneration. *Neuron*. 43:57–67.
- Sato, S., M. Ito, T. Ito, and K. Yoshioka. 2004. Scaffold protein JSAP1 is transported to growth cones of neurites independent of JNK signaling pathways in PC12h cells. *Gene*. 329:51–60.
- Schmied, R., and R.T. Ambron. 1997. A nuclear localization signal targets proteins to the retrograde transport system, thereby evading uptake into organelles in aplasia axons. *J. Neurobiol.* 33:151–160.
- Scott, M.G., E. Le Rouzic, A. Perianin, V. Pierotti, H. Enslin, S. Benichou, S. Marullo, and A. Benmerah. 2002. Differential nucleocytoplasmic shuttling of beta-arrestins. Characterization of a leucine-rich nuclear export signal in beta-arrestin2. *J. Biol. Chem.* 277:37693–37701.
- Setou, M., D.H. Seog, Y. Tanaka, Y. Kanai, Y. Takei, M. Kawagishi, and N. Hirokawa. 2002. Glutamate-receptor-interacting protein GRIP1 directly steers kinesin to dendrites. *Nature*. 417:83–87.
- Shao, Y., W. Akmentin, J.J. Toledo-Aral, J. Rosenbaum, G. Valdez, J.B. Cabot, B.S. Hilbush, and S. Halegoua. 2002. Pincher, a pinocytic chaperone for nerve growth factor/TrkA signaling endosomes. *J. Cell Biol.* 157:679–691.
- Sheu, J.Y., D.J. Kulhanek, and F.P. Eckenstein. 2000. Differential patterns of ERK and STAT3 phosphorylation after sciatic nerve transection in the rat. *Exp. Neurol.* 166:392–402.
- Shubayev, V.I., and R.R. Myers. 2001. Axonal transport of TNF-alpha in painful neuropathy: distribution of ligand tracer and TNF receptors. *J. Neuroimmunol.* 114:48–56.
- Slot, J.W., H.J. Geuze, S. Gigengack, G.E. Lienhard, and D.E. James. 1991. Immunolocalization of the insulin regulatable glucose transporter in brown adipose tissue of the rat. *J. Cell Biol.* 113:123–135.
- Sung, Y.J., M. Povelones, and R.T. Ambron. 2001. RISK-1: a novel MAPK homologue in axoplasm that is activated and retrogradely transported after nerve injury. *J. Neurobiol.* 47:67–79.
- Sung, Y.J., E.T. Walters, and R.T. Ambron. 2004. A neuronal isoform of protein kinase G couples mitogen-activated protein kinase nuclear import to axotomy-induced long-term hyperexcitability in *Aplysia* sensory neurons. *J. Neurosci.* 24:7583–7595.
- Tsukita, S., and H. Ishikawa. 1980. The movement of membranous organelles in axons. Electron microscopic identification of anterogradely and retrogradely transported organelles. *J. Cell Biol.* 84:513–530.
- Verhey, K.J., D. Meyer, R. Deehan, J. Blenis, B.J. Schnapp, T.A. Rapoport, and B. Margolis. 2001. Cargo of kinesin identified as JIP scaffolding proteins and associated signaling molecules. *J. Cell Biol.* 152:959–970.
- Wellmann, H., B. Kaltschmidt, and C. Kaltschmidt. 2001. Retrograde transport of transcription factor NF-kappa B in living neurons. *J. Biol. Chem.* 276: 11821–11829.
- Whitmarsh, A.J., C.Y. Kuan, N.J. Kennedy, N. Kelkar, T.F. Haydar, J.P. Mordes, M. Appel, A.A. Rossini, S.N. Jones, R.A. Flavell, et al. 2001. Requirement of the JIP1 scaffold protein for stress-induced JNK activation. *Genes Dev.* 15:2421–2432.
- Xia, C.H., E.A. Roberts, L.S. Her, X. Liu, D.S. Williams, D.W. Cleveland, and L.S. Goldstein. 2003. Abnormal neurofilament transport caused by targeted disruption of neuronal kinesin heavy chain KIF5A. *J. Cell Biol.* 161:55–66.
- Yang, D.D., C.Y. Kuan, A.J. Whitmarsh, M. Rincon, T.S. Zheng, R.J. Davis, P. Rakic, and R.A. Flavell. 1997. Absence of excitotoxicity-induced apoptosis in the hippocampus of mice lacking the Jnk3 gene. *Nature*. 389: 865–870.
- Yano, H., F.S. Lee, H. Kong, J. Chuang, J. Arevalo, P. Perez, C. Sung, and M.V. Chao. 2001. Association of Trk neurotrophin receptors with components of the cytoplasmic dynein motor. *J. Neurosci.* 21:RC125.
- Yasuda, J., A.J. Whitmarsh, J. Cavanagh, M. Sharma, and R.J. Davis. 1999. The JIP group of mitogen-activated protein kinase scaffold proteins. *Mol. Cell. Biol.* 19:7245–7254.